HHS Public Access

Author manuscript

Hepatology. Author manuscript; available in PMC 2017 September 01.

Published in final edited form as:

Hepatology. 2016 September ; 64(3): 880–893. doi:10.1002/hep.28599.

The toxin biliatresone causes mouse extrahepatic cholangiocyte damage and fibrosis via decreased glutathione and SOX17

Orith Waisbourd-Zinman[1], **Hong Koh**[2,3], **Shannon Tsai**[2], **Pierre-Marie Lavrut**[2], **Christine Dang**[2,4], **Xiao Zhao**[2], **Michael Pack**[2], **Jeff Cave**[5], **Mark Hawes**[5], **Kyung A. Koo**[4], **John R. Porter**[4], and **Rebecca G. Wells**[2]

[1]Division of Gastroenterology, Hepatology and Nutrition, The Children's Hospital of Philadelphia, Philadelphia, Pennsylvania

[2]Division of Gastroenterology, Department of Medicine, Perelman School of Medicine, University of Pennsylvania, Philadelphia, Pennsylvania

[3]Department of Pediatrics, Yonsei University College of Medicine, Severance Children's Hospital, Seoul, South Korea

[4]Department of Biological Sciences, University of the Sciences, Philadelphia, Pennsylvania

[5]Department of Economic Development, Jobs, Transport and Resources, Government of Victoria, Victoria, Australia

Abstract

Biliary atresia, the most common indication for pediatric liver transplantation, is a fibrotic disease of unknown etiology affecting the extrahepatic bile ducts of newborns. The recently-described toxin biliatresone causes lumen obstruction in mouse cholangiocyte spheroids and represents a new model of biliary atresia. Our aim was to determine the cellular changes caused by biliatresone in mammalian cells that ultimately lead to biliary atresia and extra-hepatic fibrosis. We treated mouse cholangiocytes in 3D spheroid culture and neonatal extra-hepatic duct explants with biliatresone and compounds that regulate glutathione. We examined the effects of biliatresone on SOX17 levels, and determined the effects of *Sox17* knockdown on cholangiocytes in 3D culture. We found that biliatresone caused disruption of cholangiocyte apical polarity and loss of monolayer integrity. Spheroids treated with biliatresone had increased permeability as shown by rhodamine efflux within 5 hours compared to untreated spheroids, which retained rhodamine for longer than 12 hours. Neonatal bile duct explants treated with the toxin showed lumen obstruction with increased subepithelial staining for α-smooth muscle actin and collagen, consistent with fibrosis. Biliatresone caused a rapid and transient decrease in glutathione, which was both necessary and sufficient to mediate its effects in cholangiocyte spheroid and bile duct explant systems. It also caused a significant decrease in in cholangiocyte levels of SOX17, and *Sox17* knockdown in cholangiocyte spheroids mimicked the effects of biliatresone.

Correspondence: Rebecca G. Wells, MD, University of Pennsylvania School of Medicine, 905 BRB II/III, 421 Curie Blvd., Philadelphia, PA 19104, Tel: 215-573-1860, Fax: 215-573-2024, rgwells@mail.med.upenn.edu.

Disclosures: All authors declare no conflict of interest

Conclusion—Biliatresone decreases glutathione and SOX17 in mouse cholangiocytes. In 3D cell systems, this leads to cholangiocyte monolayer damage and increased permeability and in extrahepatic bile duct explants it leads to disruption of the extra-hepatic biliary tree and subepithelial fibrosis. This mechanism may be important in understanding human biliary atresia.

Keywords

polarity; biliary fibrosis; cholangiocyte; α-smooth muscle actin

Biliary atresia (BA) causes rapidly progressive liver fibrosis and cirrhosis in neonates and is the primary indication for liver transplantation in children (1). Unlike in most other forms of biliary fibrosis, the initial injury in biliary atresia is most severe in the extrahepatic bile ducts (EHBD), which appear to undergo damage when fully formed, becoming completely obstructed and impeding bile flow. Surgery directly connecting the liver hilum to the bowel (*i.e.,* Kasai portoenterostomy) slows the progression of fibrosis in some children, demonstrating that the critical defect in BA is extrahepatic bile duct obstruction. BA occurs in 1:8,000–1:15,000 neonates, but the etiology remains poorly understood; familial cases are rare, and there is only limited evidence that genetic factors can cause BA. Non-random clustering of BA cases in space and time suggests that infections or toxins (2–4) may contribute to disease pathogenesis. While recent data strongly suggest that the insult to the EHBD is prenatal (5, 6), the nature of the insult and the associated cholangiocyte damage remain unknown. If the non-genetic factors that cause BA could be identified, then prevention might be possible. Similarly, a better understanding of the cellular mechanisms of BA might lead for the first time to targeted therapies.

Several animal models of BA partially recapitulate the human phenotype, but all have significant limitations. The most commonly-used model, infection of newborn BALB/c mice with rhesus rotavirus (3), has many histological and biochemical features characteristic of extrahepatic BA, but there is no definitive evidence that links rotavirus infection to human BA (7). Neonatal rat bile duct ligation also results in liver parenchymal disease similar to human BA (8, 9), but the model is technically difficult and surgical injury to extrahepatic bile ducts makes it difficult to extrapolate the resulting extrahepatic pathology to human BA. Most interestingly, *Sox17* haploinsufficient mice in certain backgrounds develop a perinatal BA-like disease and hepatitis, suggesting that reduced SOX17 levels predispose to BA (10) and raising the possibility that non-genetic factors causing such reductions in the EHBD of neonates could lead to BA.

In 1990, Australian veterinary scientists reported that outbreaks of a BA-like disease had occurred in newborn lambs in New South Wales in 1964 and 1988, both years being notable for severe droughts and the grazing of pregnant livestock on atypical flora (11, 12). Based on this work, we hypothesized that neonatal livestock were poisoned by a plant toxin ingested by their mothers. We recently reported the purification of a previously undescribed isoflavonoid, termed biliatresone, from the suspect Australian plants (*Dysphania* species), and demonstrated that this toxin causes a BA-like syndrome in larval zebrafish, with selective destruction of the EHBD (13). In mouse cholangiocytes but not hepatocytes, biliatresone also caused destabilization of microtubules, and in cholangiocyte spheroids in

3D culture, biliatresone disrupted apical polarity and caused luminal obstruction, mimicking the pathology seen in the EHBD of BA patients (13).

How biliatresone caused selective injury to the EHBD was not obvious from our initial studies. This is a critical point: since it is unlikely that pregnant women ingest biliatresone, defining the molecular mechanisms underlying the BA-like disease in zebrafish and livestock might lead to the identification of potential human teratogens that work via similar mechanisms to cause BA. We observed that biliatresone reacted strongly with glutathione (GSH). Since reduced levels of GSH cause microtubule destabilization in some cell lines (14–17), and since microtubules are essential to the maintenance of apical polarity (18), we hypothesized that biliatresone acts by lowering GSH levels, resulting in microtubule and polarity abnormalities, loss of cholangiocyte monolayer integrity, and extravasation of toxin and bile into the peri-epithelial space. Remarkably, we found that biliatresone causes transient decreases in GSH and in SOX17 in cholangiocytes in culture, and that reduced GSH is both necessary and sufficient for cholangiocyte injury and peri-epithelial fibrosis in neonatal EHBD explants. These observations suggest that any maternal toxin or stressor that reduces GSH and is excreted in neonatal bile could lead to EHBD injury.

Materials and Methods

Cell culture

A small cholangiocyte cell line was used for spheroid culture unless otherwise noted and was as described (19). Primary neonatal extrahepatic cholangiocytes were isolated by outgrowth from 0- to 3-day-old BALB/c mouse pup bile ducts as described, and were used for spheroids when specified (20). Primary cells were used at passages 1–3 for all experiments. Cells from a single litter of pups (with at least 5 animals) were used for each individual experiment with neonatal cholangiocytes. All animal work was carried out in accordance with NIH policy and approved by the Institutional Animal Care and Use Committee at the University of Pennsylvania.

Primary mouse pancreatic ductal cells were obtained from Basil Bakir and Anil Rustgi, (UPenn) and cultured in 3D as described (21). Mammary epithelial MCF-10A cells were obtained from Mauricio Reginato (Drexel University) and kidney epithelial IMCD3 cells from Katalin Susztak (UPenn) and both were cultured in 3D in a manner similar to cholangiocytes. Primary mouse enterocytes were obtained from Mary Ann Crissey and John Lynch (UPenn) and cultured in 3D as described (22, 23).

Biliatresone and compound treatments

Biliatresone was isolated as described (13, 24) from *Dysphania* species plants harvested in Australia in 2008 and shipped frozen to the United States. Cells were treated with vehicle (DMSO) or biliatresone at 2 μg/ml for up to 24 h and with BSO (100 μM, Sigma #19176), N-acetyl-L-cysteine (L-NAC) (5 μM, Sigma #A9165), N-acetyl-D-cysteine (D-NAC) (5 μM, Princeton BioMolecular Research #117600) and Sulforaphane (20 μM Sigma #S4441) as described in the text.

Spheroid culture and analysis

Primary neonatal mouse extrahepatic cholangiocytes and the small cholangiocyte cell line were cultured in 3D in a collagen-Matrigel mixture as described (13). Cholangiocytes in 3D culture replicate, polarize and form hollow spheroids, with apical markers on the luminal side and basolateral markers on the external side after 7–8 days (Supplementary Fig. 1). Spheroids were used for experiments at day 8 after plating. After treatments, cells were fixed with 4% formalin and stained for F-actin (1:1000; Phalloidin-Tetramethylrhodamine B isothiocyanate; Santa Cruz Biotechnologies 301530) or immunostained with antibodies against the integrin β-1 subunit (1:100; Abcam 95623), E-cadherin (1:100; Cell Signaling 24E10 3195S), ZO-1 (1:50; Invitrogen 40–2200), cellular tubulin (α-tubulin 1:500; Sigma-Aldrich T9026) and Ki67 (1:200; Abcam ab16667); the spheroids were imaged at the times noted. In some cases, spheroids were treated with *Sox17* siRNA (Qiagen SI01429533) or scrambled siRNA (Qiagen 1027281) as directed by the manufacturer on day 7 after plating and were evaluated on day 9. Images were obtained using a confocal microscope with 40X magnification (Leica). Pictures were taken at the level of the midsection of each spheroid, where the luminal diameter was greatest. Inserts had between 20–80 spheroids for all experiments and a minimum of 5 pictures were taken. Representative pictures are shown.

For biliatresone washout experiments, spheroids were treated with biliatresone for 24 h followed by washes and a change to media without biliatresone for an additional 24 h. For quantification of the effect of the different compounds on spheroid lumens, spheroids were stained for F-actin, and multiple confocal images were acquired and analyzed by two independent observers (O.W.-Z; H.K). Lumens were assessed as being open, closed (no lumen visible), or partially open or narrowed (small visible lumen). Only spheroids imaged at a level with a clearly visible midsection were counted.

Neonatal bile duct explant culture

Intact EHBD were isolated from 0- to 3-day-old BALB/c mice according to a protocol modified from that previously described (20). Instead of embedding the ducts in a collagen layer, ducts were placed in ice-cold V-7 cold preservation buffer (Vitron) followed by incubation with Williams E solution (Sigma), supplemented with L-glutamine and gentamicin, for 30 min at 37ºC. Biliatresone or other compounds as noted were added, and ducts were then placed on roller inserts and cultured at 37ºC in 95% O2/5% CO2 in a Vitron Dynamic Organ Culture Incubator for 1–3 days. Ducts were stained as described (25), using antibodies against the cholangiocyte marker keratin 19 (K19, 1:10, Developmental Studies Hybridoma Bank TROMAIII), α-smooth muscle actin (α-SMA; 1:1000, Sigma a2547), collagen I (1:200; Southern Biotech #1310 - 01), EDA fibronectin (1:1000; Santa Cruz sc-59826). Images were taken on a confocal microscope (Leica) at 40X. For the TUNEL assay, bile ducts were embedded in paraffin tissue and sectioned. The TUNEL stain, with a DNase-treated positive control, was performed per the manufacturers instruction's (Millipore S7110).

Glutathione measurement

GSH in cells was measured with the GSH-Glo Glutathione Assay (Promega). Cells were harvested by centrifugation, washed, re-suspended and diluted in PBS (4000–8000 cells per

well). Tissue extracts (from mouse liver and bile ducts) were washed with PBSand homogenized in PBS with EDTA (2 mM). The assay was carried out per the manufacturer's protocol. Luminescence measurements (RLU) were performed with the GloMax multi-detection system (Promega). Net GSH-dependent luminescence (net RLU) was calculated by subtracting the average luminescence of the negative control reactions (PBS). Detection of GSH by the kit is not disrupted by the interaction between biliatresone and GSH (Supplementary Fig. 2).

Rhodamine efflux assay

Assay of rhodamine efflux from spheroids, a measure of monolayer permeability, was modified from a published protocol (26). On day 8, spheroids were incubated with rhodamine 123 (100 μM; Sigma) for 15 minutes followed by 5 washes with phenol-free DMEM (Invitrogen), then were treated with either biliatresone or DMSO; live cells were imaged every 20 min 1 to 12 h post treatment using a spinning disk confocal microscope with a wide 40X lens. Permeability was quantified by examining 17 biliatresone-treated spheroids and 18 DMSO-treated spheroids imaged over the 12 h span with visual determination of loss of greater than 50% of the rhodamine was lost from the lumen. An unpaired t-test was used to compare the two groups.

RT-PCR and western blot were done *for* the small cholangiocyte cell line treated with vehicle (DMSO) or biliatresone at 2 μg/ml for 24 h and *Sox17* siRNA and scrambled siRNA (Qiagen) for 48 h. Quantitative real-time PCR (qPCR) was carried out with a Qiagen kit with the primers *RPS12*-F (ACGTCAACACTGCTCTACAAG; *RPS 12*-R CATCACAGTTGGATGCAAGC); Sox*17*-F CTCGGGGATGTAAAGGTGAA, *Sox17*-R GCTTCTCTGCCAAGGTCAAC), by the relative standard curve method. RPS12 was used as a control. For all experiments, there were 2 technical replicates, and experiments were repeated 3 times. For western blots, cells were lysed in RIPA lysis buffer (Sigma; #R0278) and 50 μg of protein from each sample was separated by SDS-PAGE, transferred to PVDF membrane 0.2 μm (Bio-Rad #162-0176), blocked with Odyssey blocking buffer (Odyssey #927-40000), incubated with primary antibodies against SOX17 (1:1000, R&D Systems #AF1924) and GAPDH (1:1000, Cell Signaling #2118) as housekeeping gene. Signals were detected using florescence on a Gel Doc system.

Statistics

Statistical significance was calculated by either the 1-tailed Student's T-test or one-way ANOVA. All experiments were done with at least 2 technical replicates and repeated at least 3 times.

Results

In the zebrafish model of biliatresone-induced BA, the intrahepatic bile ducts are spared while the EHBD are destroyed (13). Similarly, while symptomatic neonatal livestock with BA-like disease are cirrhotic (11, 12), minimally-symptomatic animals necropsied shortly after birth had marked obstruction and fibrosis of the extrahepatic bile ducts, but few

changes within the liver parenchyma (Supplementary Fig. 3). This suggested that the BA-like disease in lambs, which ultimately results in cirrhosis, begins with injury to the EHBD.

We were interested therefore in how biliatresone affects cholangiocytes, and whether its effects are specific for these cells. Our published data show that secretion of biliatresone into bile is required for toxicity (13). Consistent with localization in bile (as opposed to cholangiocyte-specific mechanisms of injury) as an explanation for selective biliary toxicity, we found that both intra- and extra-hepatic cholangiocytes, as well as multiple other ductal epithelial cells (but not enterocytes) cultured as spheroids, were equally sensitive to biliatresone, demonstrating monolayer disruption, lumen obstruction, and loss of the apical F-actin ring (13) (Fig. 1), similar to the pathology observed in the EHBD of BA patients (27). Spheroid abnormalities were not associated with changes in cholangiocyte proliferation (Supplementary Fig. 4a) and were reversible after biliatresone washout (Supplementary Fig. 5), suggesting that biliatresone did not primarily target cholangiocyte viability.

Lumen obstruction and changes in F-actin in spheroids are associated with mis- localization of the apical markers ZO-1 and E-cadherin (Fig. 2a–c). Time course studies demonstrated that this follows decreased staining for cellular tubulin, which likely reflects destabilization or depolymerization of microtubules (with the decreased staining a function of fixating and permeabilization); reduced tubulin staining is observed within 3 h of biliatresone treatment, while changes in apical polarity markers and obstruction of spheroid lumens are not seen until 6–12 h of treatment (Fig. 2c).

To determine whether changes in cell-cell adhesion markers and loss of polarity are associated with increased epithelial permeability, we assayed rhodamine efflux from cholangiocyte spheroid lumens. Rhodamine is taken up from the media at the cholangiocyte basolateral surface, transported across the cells, and then excreted apically, resulting in accumulation in the lumen. We preloaded spheroids equally with rhodamine, and then treated with either biliatresone or vehicle. Spheroids treated with vehicle retained the majority of pre-loaded rhodamine in the lumen even after 12 h. Spheroids treated with biliatresone, however, demonstrated rapid loss of luminal rhodamine, particularly within the first hour, with 50% loss in 4.4 ± 0.6 h compared to 11.4 ± 0.4 h for the DMSO treated spheroids, $p<0.0001$. This suggests that biliatresone increased cholangiocyte monolayer permeability (Fig. 3).

In the setting of increased epithelial permeability *in vivo*, cholangiocyte exposure to biliatresone could result in leakage of bile acids or biliatresone itself into the duct submucosa and deeper structures. We adapted methods used for long-term culture of precision cut liver (and other tissue) slices in a high oxygen environment(28) to the culture of isolated intact neonatal mouse EHBDs. In this explant culture system, ducts treated with biliatresone for 1 day and stained with antibodies against the cholangiocyte marker K19 demonstrated monolayer disruption with patchy lumen obstruction when compared to vehicle-treated ducts, which were uniformly completely open. TUNEL staining did not demonstrate increases in apoptosis in biliatresone-treated ducts (Supplementary Fig. 4b). Biliatresone-treated ducts also demonstrated an increase in immunostaining in periductal regions for the myofibroblast marker α-smooth muscle actin (α-SMA), and the fibrosis-

associated matrix proteins fibronectin EIIIA and type I collagen (Fig. 4). These results suggest that exposure of neonatal EHBD to biliatresone could result in ductal disruption and fibrosis, as is seen in human BA patients.

After demonstrating the effects of biliatresone on cholangiocytes in spheroid and duct explant culture, we studied its mechanism of action. We have shown that biliatresone contains an α-methylene-ketone reactive group and binds GSH strongly and rapidly (29). Given published reports that decreases in GSH in some cell types result in diminished cellular tubulin staining (14–17), as we observed in cholangiocytes after biliatresone treatment, we hypothesized that biliatresone acts through GSH. We first measured GSH levels in cholangiocytes treated with biliatresone and observed a 43.6% decrease in GSH after 1 h of treatment, with recovery over time (Fig. 5a). When we measured glutathione in tissue, we found that the EHBD had significantly less glutathione (total and reduced) than the liver in both neonates and adults, suggesting that the EHBD might be particularly susceptible to biliatresone-induced decreases in GSH (Supplementary Fig. 6), although given the lack of a significant difference in glutathione levels between neonates and adults, this would be unlikely to explain the susceptibility of neonates to BA-like diseases.

To determine the role of GSH in cholangiocyte damage resulting from biliatresone, we added compounds that increase GSH to biliatresone-treated cultures. The effects of biliatresone on cholangiocyte spheroids were prevented by co-treatment with N-acetyl-L-cysteine (L-NAC) or by pre-treatment with sulforaphane, but not by co-treatment with N-acetyl-D-cysteine (D-NAC) (Fig. 5b–d). Sulforaphane is an Nrf2 activator that increases GSH (30). L-NAC and D-NAC are both anti-oxidants and bind biliatresone equivalently, but only L-NAC increases GSH synthesis, suggesting that the effects of L-NAC are mediated by increased GSH rather than by sequestering biliatresone (31, 32). We quantified the effects of the different compounds by grading spheroid lumens as open, partially open or closed, and confirmed that lumen patency was influenced by GSH levels (Fig. 5d).

To determine whether decreased GSH is both a necessary and sufficient mediator of biliatresone effects, we treated cholangiocyte spheroids and neonatal mouse EHBD explants with buthionine sulfoximine (BSO), which inhibits γ-glutamylcysteine synthetase, the enzyme that mediates the first step in GSH synthesis. BSO, like biliatresone, caused a rapid decrease in GSH in cholangiocytes (Fig. 6a). Decreasing GSH with BSO mimicked the effects of biliatresone, with lumen obstruction and disrupted polarity in spheroids, and lumen narrowing and increased periductal α-SMA, in EHBD explants (Fig. 5a–e). BSO, similarly to biliatresone, resulted in decreased immunostaining for cellular tubulin, and this change was prevented with L-NAC and sulforaphane treatment but not D-NAC. The sequence of events observed in cholangiocyte spheroids after BSO treatment (decreased tubulin staining followed by mislocalization of polarity markers and lumen closure) was the same as that observed for biliatresone (Fig. 6b,c). In addition, BSO treatment for 1 h followed by incubation with BSO-free media showed that spheroids appeared damaged at 12 h, but after a 24 h washout polarity was restored and lumens reformed (Fig. 6b). These data suggested that the effects of BSO, like those of biliatresone, are reversible in the spheroid model (Fig. 6c and Supplementary Fig. 5).

In addition to investigating the role of GSH in biliatresone effects, we studied the role of the transcription factor SOX17. A BA-like phenotype including loss of integrity of the ductal epithelial monolayer is seen in *Sox17* haploinsufficient mice in certain genetic backgrounds (10). To determine whether SOX17 expression is affected by biliatresone, we examined SOX17 levels in cholangiocytes after biliatresone treatment. *Sox17* mRNA and protein levels were reduced significantly following biliatresone treatment (Fig. 7a,b). To determine whether decreases in SOX17 mimicked the effects of biliatresone in our cholangiocyte model system, we silenced *Sox17* by siRNA treatment, achieving 95% knockdown, as confirmed by quantitative RT-PCR and immunohistochemistry (Supplementary Fig. 7). Treatment with *Sox17* siRNA but not scrambled siRNA resulted in lumen obstruction and apical tight junction disruption, mimicking the effects of biliatresone (Fig. 7 and Supplementary Video 1). *Sox17* siRNA treatment resulted in the same sequence of events in spheroids (taking into account approximately 24 h required for *Sox17* knockdown after transfection) as seen for biliatresone and BSO, with decreased staining for cellular tubulin occurring first, followed by loss of apical polarity and lumen obstruction (Fig. 7d). Overexpression of SOX17 by transfection of a cDNA encoding *Sox17* resulted in spheroid disruption in both the presence and absence of biliatresone, suggesting that SOX17 levels are tightly controlled, and preventing us from carrying out rescue experiments. Silencing of *Sox17* had no effect on GSH levels (Fig. 7e), suggesting that decreases in SOX17 were either caused by GSH reductions or in a parallel pathway.

Discussion

The etiology of BA is unknown, although epidemiological studies support an infection or toxin exposure, likely occurring prenatally (5, 6), in the setting of genetic susceptibility (4, 33–36). Our group recently identified an isoflavonoid called biliatresone which has been implicated in outbreaks of a BA-like syndrome in Australian livestock and which also causes selective EHBD destruction in zebrafish (13). This is important evidence supporting the hypothesis that toxins can cause BA. Here we used cultured cholangiocyte spheroids and a novel bile duct explant culture system to delineate the effects of biliatresone, showing that biliatresone disrupts the cholangiocyte monolayer and, in duct explants, causes peri-epithelial fibrosis. We identify decreases in GSH and SOX17 as key mediators of these effects and demonstrate that decreased GSH independent of biliatresone causes duct explant obstruction and fibrosis. Our data suggest that environmental agents that reduce GSH and that reach the neonatal bile duct might cause BA. Redox stress is also a contributing factor in biliatresone-induced cholangiocyte injury in zebrafish, although unlike in our mammalian cell systems, decreased glutathione potentiates but is not sufficient for injury (Zhao et al., unpublished).

A decrease in GSH was sufficient for cholangiocyte injury in our model systems. GSH levels rapidly decline after biliatresone treatment, although there is partial restoration over time. BSO similarly causes rapid decreases in cholangiocyte GSH, and the time course of injury after follows the same sequence of events as for biliatresone. BSO causes damage in spheroids even after a 1 h exposure, but spheroids recover after a 24 h washout. Bile ducts treated with DMSO and biliatresone demonstrated no difference in apoptosis or proliferation, though it is likely that apoptosis occurs later in the process. This suggests the

possibility that a potentially transient insult to the bile ducts could cause significant damage, but also that cholangiocyte recovery could occur *in vivo* if the injury were stopped. These findings may have important implications for human disease. Although there is no evidence that pregnant women are exposed to biliatresone itself, humans may be exposed to other GSH-depleting molecules, and it is conceivable that some of these cross the placenta and are excreted in neonatal bile.

One of the first signs of injury we observe in cholangiocyte spheroids is a decrease in cellular tubulin immunoreactivity. Microtubule disruption caused by decreases in GSH has been described in other cell types including colonic, kidney and neuronal cells (14–17), and our data suggest that microtubule changes in cholangiocyte spheroids are the result of decreased GSH after biliatresone treatment. Microtubules play an important role in lumen formation and the maintenance of polarity in several types of epithelial cells, including cholangiocytes (18, 26). In biliatresone-mediated cholangiocyte injury, changes in cellular tubulin occur after and as a result of a decrease in GSH and are accompanied by loss of cell-to-cell adhesion and increased epithelial permeability. Polarity abnormalities have been reported in human BA: a recent study found that extracellular matrix proteins and adhesion molecules which mediate cellular polarity and integrity are abnormal in BA patients (37). Additionally, in zebrafish it was shown that that planar cell polarity plays an important role invertebrate biliary development (38).

The importance of the epithelium in preventing injuries and the injury response has been studied in the lung, where loss of bronchial epithelial cell integrity leads to inflammation and fibrosis (39, 40). We observed increased epithelial permeability after biliatresone treatment. Similar damage to the cholangiocyte monolayer in bile ducts could potentially result in leakage of both bile and biliatresone into the peri-ductular tissues, either of which could potentially cause myofibroblast activation and fibrosis. Our finding that biliatresone exposure causes increased α-SMA and collagen expression in the EHBD explant culture system is consistent with both indirect and direct effects of biliatresone on myofibroblast precursor cells. In this context, it is interesting that biliatresone-mediated injuries in cholangiocyte spheroids are reversible. We speculate that cholangiocytes could recover from an initial injury, but that the exposure of the submucosal and deeper structures to bile (or biliatresone or similar toxins) might lead to more permanent damage. Obstruction could potentially be secondary to cholangiocyte injury, associated inflammation, or a secondary fibrotic process.

Another potential cause of bile duct obstruction is epithelial deciduation, which is observed in *Sox17* heterozygote mice that develop a BA-like syndrome (10). In these mice, SOX17 is required to maintain the epithelial architecture of the gallbladder and cystic duct. We find that biliatresone reduces SOX17 in cholangiocytes, and that silencing *Sox17* mimics the effects of biliatresone on the biliary epithelium. SOX17 has been implicated as key protein in the development of the EHBD (41), and our model suggests that it is important to duct maintenance as well.

One of the key questions in BA research is why early manifestations in humans are relatively selective for the EHBD. Using spheroid culture systems, we found that multiple ductular

epithelial cells, including mammary ductal, pancreatic ductal, and kidney tubular cells were affected by biliatresone; enterocytes, which are epithelial cells but not ductular, were not affected. Similarly, we found that intra- and extrahepatic cholangiocytes *in vitro* appear to be equally susceptible to injury. These findings raise interesting questions about the specificity of biliatresone for extrahepatic cholangiocytes in zebrafish and livestock. It appears likely that biliatresone is toxic to many cells, but that *in vivo* it is selective for extra-hepatic cholangiocytes because of excretion and/or concentration in bile. In support of this hypothesis, we found in zebrafish that intrahepatic bile ducts are required for biliatresone toxicity. We speculate that biliatresone crosses the placenta and enters the fetal liver and the biliary system; maternal hepatic metabolism may prevent cholangiocyte exposure in the mother. The stasis of bile *in utero* as well as concentration of bile and biliatresone in the gallbladder might explain EHBD toxicity. We hypothesize that biliatresone undergoes metabolism by hepatocytes and that there may be significant differences in metabolism between neonatal and adult livers. Further studies will be needed to answer this question. Low levels of GSH may also predispose the EHBD to injury. We previously reported that hepatocytes are resistant to the effects of biliatresone (13). GSH levels in the liver parenchyma are higher than in the EHBD, which may protect hepatocytes, although there is no difference in GSH levels between adult and neonatal mouse EHBDs, highlighting the potential importance of late fetal or neonatal vs. adult hepatic transport and metabolism of biliatresone. The GSH levels of intrahepatic compared to extrahepatic cholangiocytes are unknown but could potentially account for selective extrahepatic toxicity. Finally, it is possible that both intra- and extra-hepatic cholangiocytes are injured by biliatresone, but that the regenerative abilities of the liver compared to the EHBD result in repair after injury rather than fibrosis.

There is a wealth of data implicating both immune dysregulation and genetic factors in human BA. Toxin-induced BA is not inconsistent with these findings, and may represent a primary injury, with immune dysregulation representing a secondary insult. Ongoing studies are focused on determining links between biliatresone treatment and immune dysregulation.

In summary, our findings are consistent with a model of biliatresone-induced injury that includes primary injury to the EHBDs, loss of cell-to-cell adhesion, cholangiocyte polarity changes, increased epithelial permeability, and resulting myofibroblast activation and fibrosis. These events are secondary to reductions in GSH and are accompanied by reduced SOX17. Elements of this model, including the role of GSH, the potentially transient nature of the insult, the increase in epithelial permeability, and the reversibility of cholangiocyte damage, may provide important insights into both the pathogenesis and clinical course of human BA and may lead to the development of new preventive measures or novel treatments in the future.

Supplementary Material

Refer to Web version on PubMed Central for supplementary material.

Acknowledgments

Grant Support:

This research was supported by NIH/NIDDK grants R01 DK092111 to R.G.W, M.P., and J.R.P., and 5T32 HD043021-10 and 1T32 DK101371-01 to O.W.-Z., by an AASLD

Advanced Hepatology and Liver Transplant Fellowship grant to O.W.-Z., and by grants from the Fred and Suzanne Biesecker Pediatric Liver Center to R.G.W. and M.P.

The authors are grateful to Basil Bakir, Anil Rustgi, Mauricio Reginato, Katalin Susztak, Mary Ann Crissey and John Lynch for providing cells, and to the Cell and Developmental Biology Microscopy core and the NIDDK Center for Molecular Studies in Digestive and Liver Disease Molecular Pathology and Imagine Core (P30 DK050306) at the University of Pennsylvania for imaging support.

Abbreviations

BA	biliary atresia
BSO	DL-buthionine sulfoximine
D-NAC	N-acetyl-D-cysteine
EHBD	extra hepatic bile ducts
GSH	glutathione
L-NAC	N-acetyl-L-cysteine

References

Author names in bold designate shared co-first authorship

1. Haber BA, Russo P. Biliary atresia. Gastroenterol Clin North Am. 2003; 32:891–911. [PubMed: 14562580]
2. Bezerra JA. Potential etiologies of biliary atresia. Pediatr Transplant. 2005; 9:646–651. [PubMed: 16176425]
3. Riepenhoff-Talty M, Schaekel K, Clark HF, Mueller W, Uhnoo I, Rossi T, et al. Group A rotaviruses produce extrahepatic biliary obstruction in orally inoculated newborn mice. Pediatr Res. 1993; 33:394–399. [PubMed: 8386833]
4. Tiao MM, Tsai SS, Kuo HW, Chen CL, Yang CY. Epidemiological features of biliary atresia in Taiwan, a national study 1996–2003. J Gastroenterol Hepatol. 2008; 23:62–66. [PubMed: 17725591]
5. Harpavat S, Finegold MJ, Karpen SJ. Patients with biliary atresia have elevated direct/conjugated bilirubin levels shortly after birth. Pediatrics. 2011; 128:e1428–1433. [PubMed: 22106076]
6. Zhou K, Lin N, Xiao Y, Wang Y, Wen J, Zou GM, et al. Elevated bile acids in newborns with Biliary Atresia (BA). PLoS One. 2012; 7:e49270. [PubMed: 23166626]
7. Hertel PM, Estes MK. Rotavirus and biliary atresia: can causation be proven? Curr Opin Gastroenterol. 2012; 28:10–17. [PubMed: 22123643]
8. Gibelli NE, Tannuri U, de Mello ES, Rodrigues CJ. Bile duct ligation in neonatal rats: is it a valid experimental model for biliary atresia studies? Pediatr Transplant. 2009; 13:81–87. [PubMed: 18452497]
9. Holder TM, Ashcraft KW. Production of experimental biliary atresia by ligation of the common bile duct in the fetus. Surg Forum. 1966; 17:356–357. [PubMed: 5920960]
10. Uemura M, Ozawa A, Nagata T, Kurasawa K, Tsunekawa N, Nobuhisa I, et al. Sox17 haploinsufficiency results in perinatal biliary atresia and hepatitis in C57BL/6 background mice. Development. 2013; 140:639–648. [PubMed: 23293295]
11. Harper P, Plant JW, Unger DB. Congenital biliary atresia and jaundice in lambs and calves. Aust Vet J. 1990; 67:18–22. [PubMed: 2334368]

12. Robson, S. New South Wales Animal Health Surveillance. NSW Department of Primary Industries; Sydney, New South Wales, Australia: Congenital biliary atresia and jaundice in lambs. Sect. 2–4
13. Lorent K, Gong W, Koo KA, Waisbourd-Zinman O, Karjoo S, Zhao X, et al. Identification of a plant isoflavonoid that causes biliary atresia. Sci Transl Med. 2015; 7:286ra267.
14. Aquilano K, Baldelli S, Cardaci S, Rotilio G, Ciriolo MR. Nitric oxide is the primary mediator of cytotoxicity induced by GSH depletion in neuronal cells. J Cell Sci. 2011; 124:1043–1054. [PubMed: 21363890]
15. Hosono T, Hosono-Fukao T, Inada K, Tanaka R, Yamada H, Iitsuka Y, et al. Alkenyl group is responsible for the disruption of microtubule network formation in human colon cancer cell line HT-29 cells. Carcinogenesis. 2008; 29:1400–1406. [PubMed: 18515280]
16. Huang X, Chen L, Liu W, Qiao Q, Wu K, Wen J, et al. Involvement of oxidative stress and cytoskeletal disruption in microcystin-induced apoptosis in CIK cells. Aquat Toxicol. 2015; 165:41–50. [PubMed: 26022555]
17. Zuelke KA, Jones DP, Perreault SD. Glutathione oxidation is associated with altered microtubule function and disrupted fertilization in mature hamster oocytes. Biol Reprod. 1997; 57:1413–1419. [PubMed: 9408248]
18. Akhtar N, Streuli CH. An integrin-ILK-microtubule network orients cell polarity and lumen formation in glandular epithelium. Nat Cell Biol. 2013; 15:17–27. [PubMed: 23263281]
19. Ueno Y, Alpini G, Yahagi K, Kanno N, Moritoki Y, Fukushima K, et al. Evaluation of differential gene expression by microarray analysis in small and large cholangiocytes isolated from normal mice. Liver Int. 2003; 23:449–459. [PubMed: 14986819]
20. Karjoo S, Wells RG. Isolation of neonatal extrahepatic cholangiocytes. J Vis Exp. 2014
21. Reichert M, Takano S, Heeg S, Bakir B, Botta GP, Rustgi AK. Isolation, culture and genetic manipulation of mouse pancreatic ductal cells. Nat Protoc. 2013; 8:1354–1365. [PubMed: 23787893]
22. Sato T, Vries RG, Snippert HJ, van de Wetering M, Barker N, Stange DE, et al. Single Lgr5 stem cells build crypt-villus structures in vitro without a mesenchymal niche. Nature. 2009; 459:262–265. [PubMed: 19329995]
23. Muzumdar MD, Tasic B, Miyamichi K, Li L, Luo L. A global double-fluorescent Cre reporter mouse. Genesis. 2007; 45:593–605. [PubMed: 17868096]
24. Koo KA, Lorent K, Gong W, Windsor P, Whittaker SJ, Pack M, et al. Biliatresone, a Reactive Natural Toxin from Dysphania glomulifera and D. littoralis: Discovery of the Toxic Moiety 1,2-Diaryl-2-Propenone. Chem Res Toxicol. 2015; 28:1519–1521. [PubMed: 26175131]
25. Dipaola F, Shivakumar P, Pfister J, Walters S, Sabla G, Bezerra JA. Identification of intramural epithelial networks linked to peribiliary glands that express progenitor cell markers and proliferate after injury in mice. Hepatology. 2013; 58:1486–1496. [PubMed: 23703727]
26. Tanimizu N, Miyajima A, Mostov KE. Liver progenitor cells fold up a cell monolayer into a double-layered structure during tubular morphogenesis. Mol Biol Cell. 2009; 20:2486–2494. [PubMed: 19297530]
27. Diaz R, Kim JW, Hui JJ, Li Z, Swain GP, Fong KS, et al. Evidence for the epithelial to mesenchymal transition in biliary atresia fibrosis. Hum Pathol. 2008; 39:102–115. [PubMed: 17900655]
28. Klassen LW, Thiele GM, Duryee MJ, Schaffert CS, DeVeney AL, Hunter CD, et al. An in vitro method of alcoholic liver injury using precision-cut liver slices from rats. Biochem Pharmacol. 2008; 76:426–436. [PubMed: 18599023]
29. Koo K, Waisbourd-Zinman O, Wells R, Pack M, Porter JR. Reactivity of Biliatresone, a Natural Biliary Toxin, with Glutathione, Histamine and Amino Acids. Chem Res Toxicol. 2015
30. Steele ML, Fuller S, Patel M, Kersaitis C, Ooi L, Munch G. Effect of Nrf2 activators on release of glutathione, cysteinylglycine and homocysteine by human U373 astroglial cells. Redox Biol. 2013; 1:441–445. [PubMed: 24191238]
31. Sarnstrand B, Tunek A, Sjodin K, Hallberg A. Effects of N-acetylcysteine stereoisomers on oxygen-induced lung injury in rats. Chem Biol Interact. 1995; 94:157–164. [PubMed: 7828222]

32. Karg E, Tunek A, Brotell H, Rosengren E, Rorsman H. Alteration of glutathione level in human melanoma cells: effect of N-acetyl-L-cysteine and its analogues. Pigment Cell Res. 1990; 3:11–15. [PubMed: 2377577]
33. Garcia-Barceló M-M, Yeung M-Y, Miao X-P, Tang CS-M, Chen G, So M-T, et al. Genome-wide association study identifies a susceptibility locus for biliary atresia on 10q24.2. Human Molecular Genetics. 2010; 19:2917–2925. [PubMed: 20460270]
34. Leyva-Vega M, Gerfen J, Thiel BD, Jurkiewicz D, Rand EB, Pawlowska J, et al. Genomic alterations in biliary atresia suggest region of potential disease susceptibility in 2q37.3. Am J Med Genet A. 2010; 152a:886–895. [PubMed: 20358598]
35. Rurarz M, Czubkowski P, Chrzanowska K, Cielecka-Kuszyk J, Marczak A, Kaminska D, et al. Biliary atresia in children with aberrations involving chromosome 11q. J Pediatr Gastroenterol Nutr. 2014; 58:e26–29. [PubMed: 23752074]
36. Tsai EA, Grochowski CM, Loomes KM, Bessho K, Hakonarson H, Bezerra JA, et al. Replication of a GWAS signal in a Caucasian population implicates ADD3 in susceptibility to biliary atresia. Hum Genet. 2014; 133:235–243. [PubMed: 24104524]
37. Whitby T, Schroeder D, Kim HS, Petersen C, Dirsch O, Baumann U, et al. Modifications in integrin expression and extracellular matrix composition in children with biliary atresia. Klin Padiatr. 2015; 227:15–22. [PubMed: 25565194]
38. Cui S, Capecci LM, Matthews RP. Disruption of planar cell polarity activity leads to developmental biliary defects. Dev Biol. 2011; 351:229–241. [PubMed: 21215262]
39. Eurlings IM, Reynaert NL, van den Beucken T, Gosker HR, de Theije CC, Verhamme FM, et al. Cigarette smoke extract induces a phenotypic shift in epithelial cells; involvement of HIF1alpha in mesenchymal transition. PLoS One. 2014; 9:e107757. [PubMed: 25329389]
40. Gao W, Li L, Wang Y, Zhang S, Adcock IM, Barnes PJ, et al. Bronchial epithelial cells: The key effector cells in the pathogenesis of chronic obstructive pulmonary disease? Respirology. 2015; 20:722–729. [PubMed: 25868842]
41. Spence JR, Lange AW, Lin SC, Kaestner KH, Lowy AM, Kim I, et al. Sox17 regulates organ lineage segregation of ventral foregut progenitor cells. Dev Cell. 2009; 17:62–74. [PubMed: 19619492]

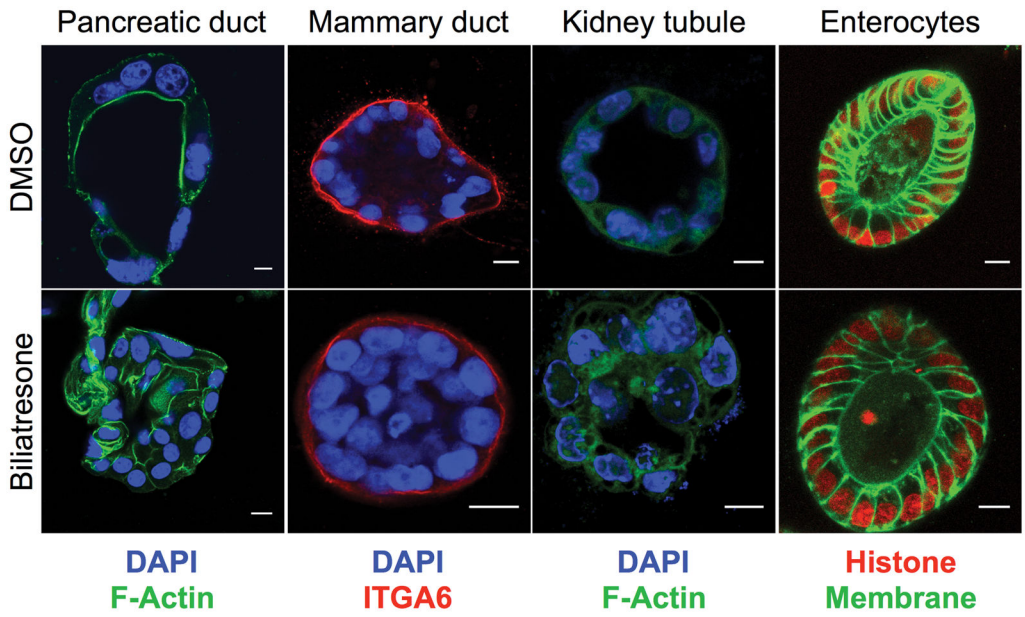

Figure 1. Multiple ductular cells are sensitive to biliatresone

Primary mouse pancreatic ductal cells, MCF-10A mammary ductal epithelial cells, IMCD3 renal tubule epithelial cells, and primary mouse enterocytes were cultured in 3D until they formed spheroids, then treated with vehicle (DMSO) or biliatresone for 24 h and stained as noted for F-actin (green) or integrin α6 (ITGA6; red). Enterocytes are from transgenic mice labeled with GFP (membrane targeted; green) and mCherry (labeled histone; red). DAPI nuclear stain (blue). Treatment of all cell types except enterocytes with biliatresone resulted in loss of the spheroid monolayer and lumens, similar to what was observed for cholangiocytes. Representative of 3 independent experiments, each with 2 technical replicates.

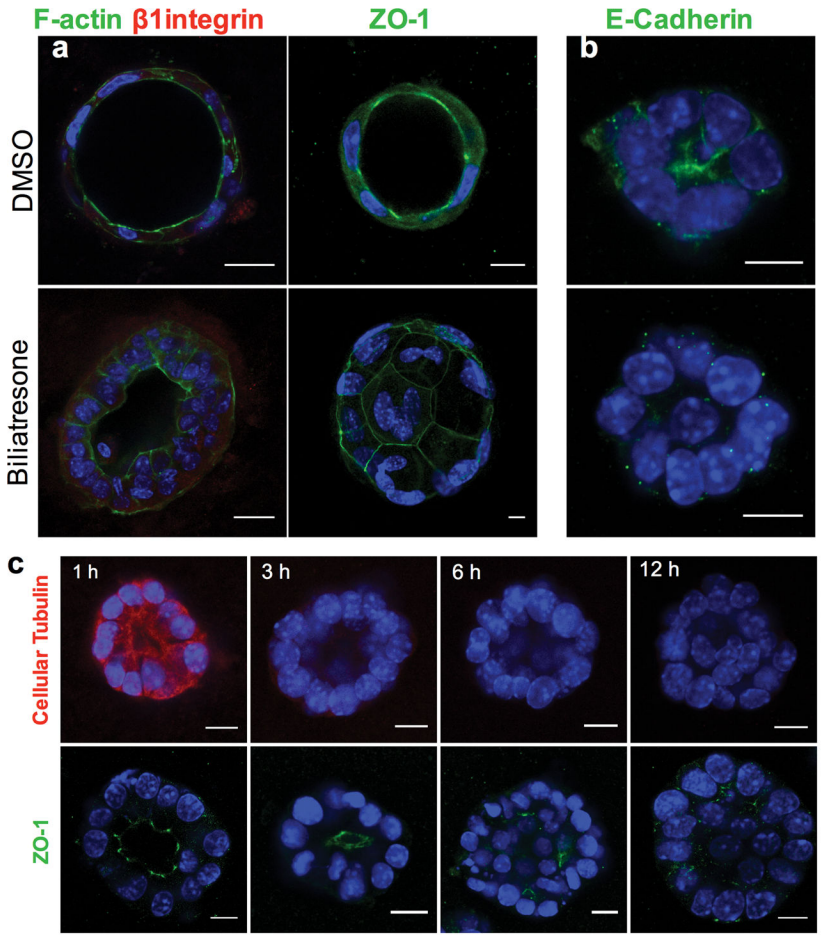

Figure 2. Biliatresone causes destabilization of cellular tubulin and loss of cholangiocyte polarity

Primary neonatal mouse cholangiocytes in spheroid culture were treated with vehicle (DMSO) or biliatresone for 24 h and immunostained for F-actin (green), the β1 integrin subunit (red), or ZO-1 (green) as indicated. b) A cholangiocyte cell line was treated similarly and immunostained for E-cadherin (green). c) Cholangiocyte cell line spheroids were treated with biliatresone for 1–12 h and immunostained for cellular tubulin (red) or ZO-1 (green). In all cases nuclei were stained with DAPI (blue). Scale bars, 10 μm. Representative images from 3 independent experiments, each experiment carried out in duplicate. BD – bile duct, PT – portal tract, EHBD – extra-hepatic bile duct

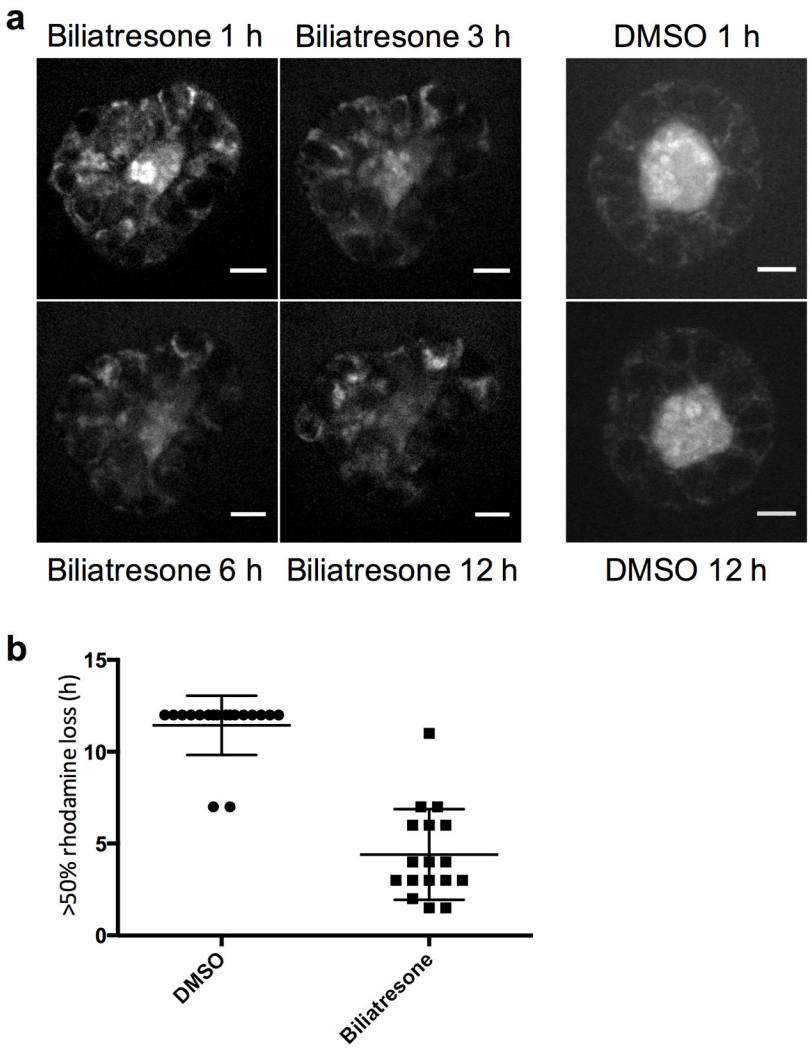

Figure 3. Biliatresone causes epithelial leakiness

Cholangiocyte spheroids were loaded with rhodamine, treated with vehicle (DMSO) or biliatresone for 12 h, and imaged every 20 min. (a) Representative spheroids at the times indicated. (b) Quantification of rhodamine loss from spheroids over 12 h. N=17 (biliatresone) and 18 (DMSO), from 6 independent experiments. The time at which >50% of luminal signal was lost was scored. Mean ± SD shown, $p<0.0001$. Scale bar is 10 μm.

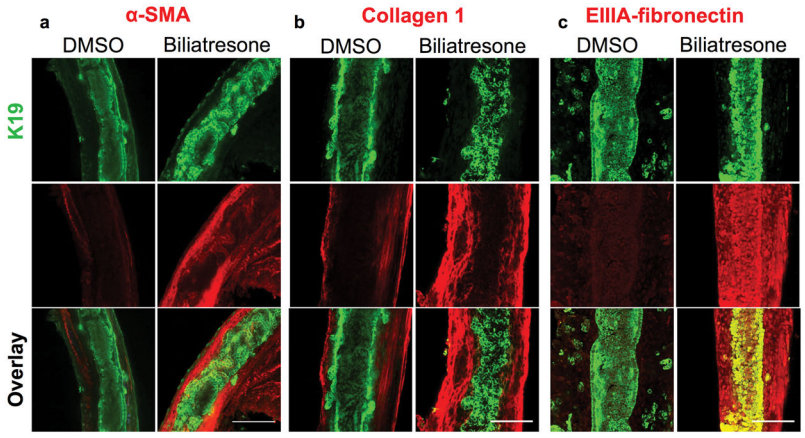

Figure 4. Biliatresone causes monolayer disruption, patchy obstruction, myofibroblast activation and fibrosis in neonatal EHBD explant cultures

Immunofluorescence staining of neonatal mouse EHBD incubated for 24 h with biliatresone or vehicle (DMSO) and stained for the cholangiocyte marker K19 (green) and (a) the myofibroblast marker α-SMA (red), and the fibrosis markers (b) collagen 1 (red), or (c) EIIIA-fibronectin (red). K19 staining demonstrates ductal disruption, while the other stains demonstrate myofibroblast accumulation and matrix deposition in the submucosal and other periductal regions with biliatresone treatment. Representative of (a) 7 independent experiments with 13 ducts of each condition, (b) 3 independent experiment with 6 ducts and (c) 3 independent experiments with 6 ducts. Scale bar, 100 μm.

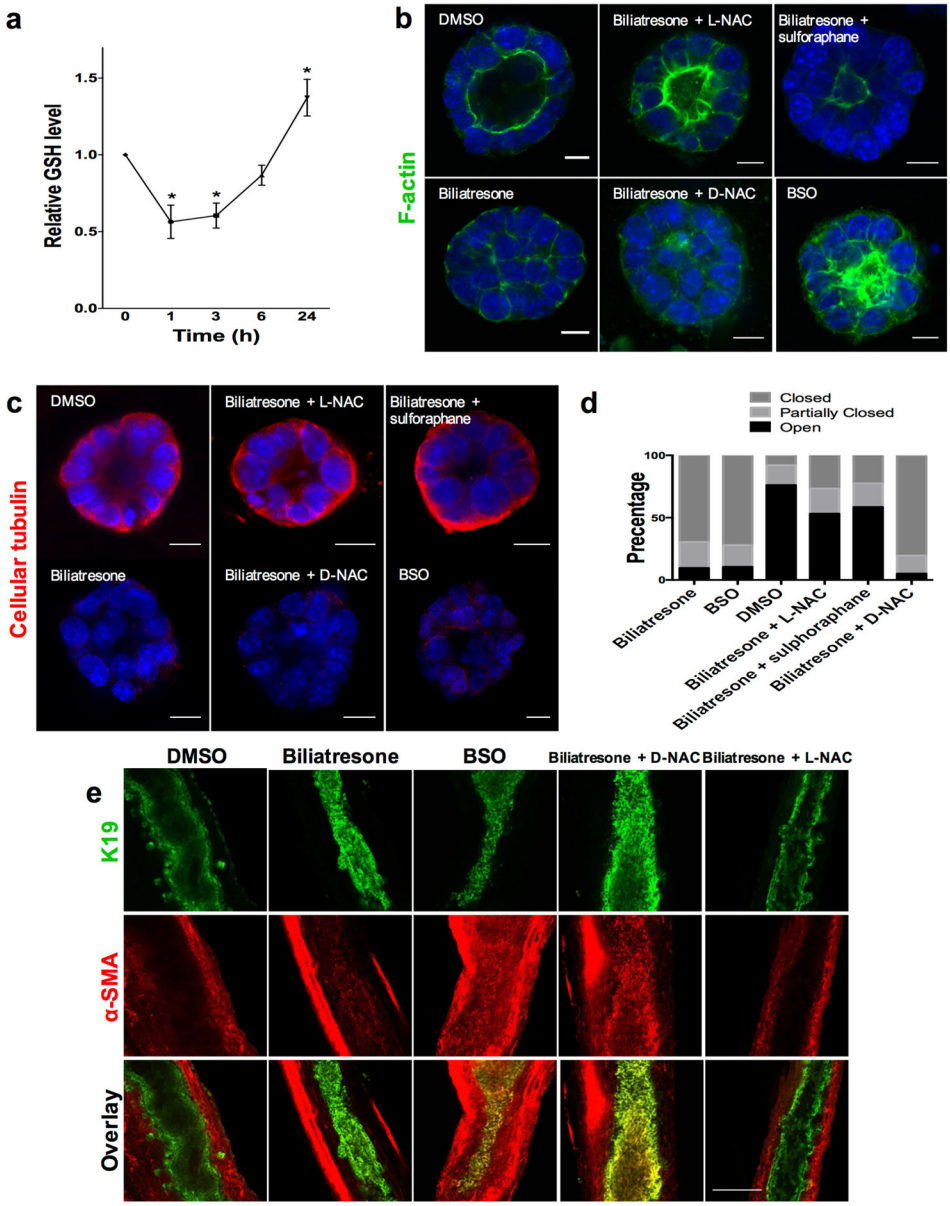

Figure 5. The effects of biliatresone are secondary to decreased GSH

(a) GSH levels were measured in cholangiocytes in 2D culture over 24 h following treatment with biliatresone. Mean ± SEM, *, $p<0.05$ (compared to 0 time point). (b) Cholangiocyte spheroids in 3D culture were treated with the compounds indicated for 24 h and were then immunostained for F-actin (green) and with the nuclear stain DAPI (blue). Only spheroids that were fully visualized along the z axis were scored. (c) Spheroids treated as in a, immunostained for cellular tubulin (red). d) Quantification of the spheroids from a. Spheroids (96–119) in three different experiments for each condition were graded as open (lumen wide open), partially closed (small lumen), or closed (obstructed lumen). e) Immunofluorescence staining of neonatal mouse extrahepatic bile ducts incubated for 24 h in high oxygen environment (see methods), treated with the compounds indicated and immunostained for K19 (green) and α-SMA (red). Size bars for a,b: 10 μM; for e: 100 μM.

Representative images from (a,b), 3 independent experiments, each experiment done in duplicate. (e) from 4 independent experiments with at least 8 ducts total for each condition.

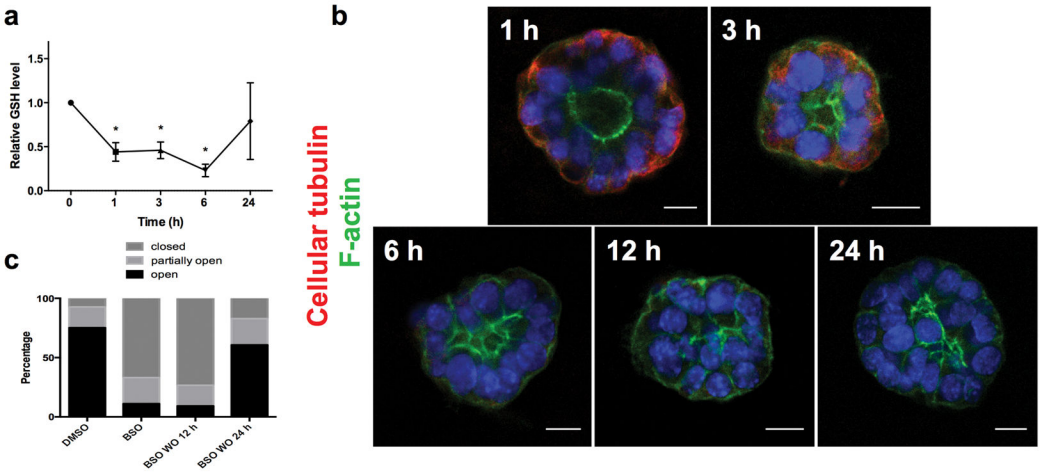

Figure 6. GSH reduction causes transient cholangiocyte spheroid disruption

(a) GSH levels were measured in cholangiocytes in 2D culture over 24 h following treatment with BSO. Mean ± SEM, *p<0.05 compared to 0 time point. Representative of 3 independent experiments each with duplicates.

(b) Cholangiocyte spheroids were treated with BSO for 1–24 h as indicated, then stained for F-actin (green) and β1 integrin (red). DAPI nuclear stain (blue). Cellular tubulin changes, F-actin redistribution, monolayer disruption, and loss of lumens followed same sequence and time course as for biliatresone. Scale bar, 10 μm. (c) Spheroids were treated with vehicle (DMSO) or BSO for 24 h (two left bars), or with BSO for 1 h followed by a 12 or 24 h washout period (two right bars). Lumens were scored as open, closed, or partially open as described in the methods. N=286–327 spheroids per condition.

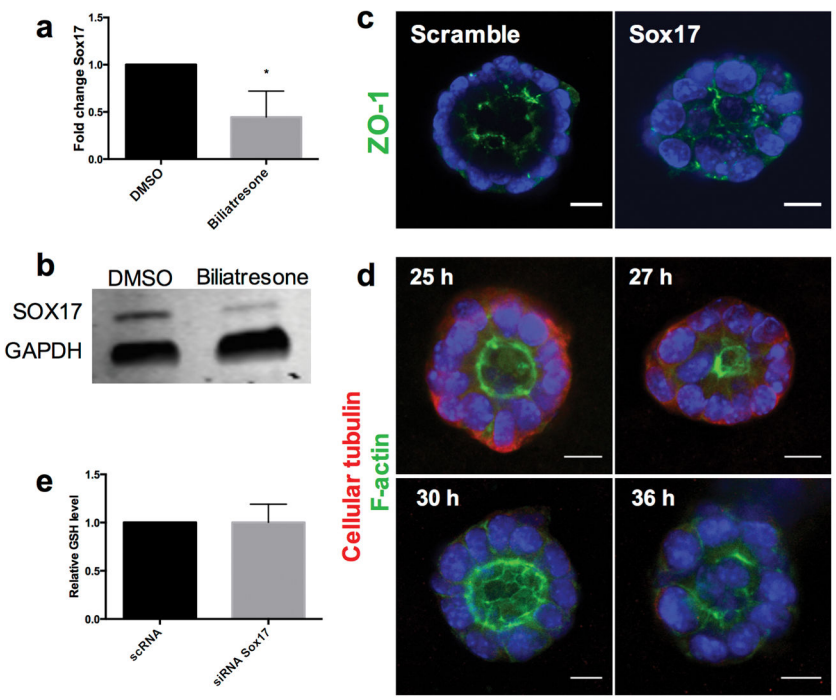

Figure 7. Biliatresone decreases SOX17 and silencing *Sox17* phenocopies the biliatresone effect

(a) *Sox17* mRNA expression in cholangiocytes in 2D culture treated with biliatresone or vehicle (DMSO) for 24 h. * $p<0.05$. (b) Western immunoblot of cholangiocytes in 2D culture treated with biliatresone or vehicle (DMSO) for 24 h. GAPDH loading control. (c) Cholangiocyte spheroids treated with siRNA for *Sox17* or with scrambled RNA for 24 h, then stained for ZO1 and with DAPI. (d) Cholangiocyte spheroids treated with siRNA for *Sox17* for the times indicated, then immunostained for F-actin (green) and cellular tubulin (red); DAPI nuclear stain (blue). (e) GSH levels in cholangiocytes in 2D culture treated with siRNA for *Sox17* or scrambled RNA, $p=0.98$. Graphs are mean ± SD. Size bars, 10 μm. Representative pictures for c and d of 3 independent experiments with duplicate wells of spheroids.